

# 1 **A coastal vulnerability assessment for planning climate resilient infrastructure.**

2  
3 Jennifer M. Brown<sup>1\*</sup>, Karyn Morrissey<sup>2,3</sup>, Philip Knight<sup>2</sup>, Thomas D. Prime<sup>1,2</sup>, Luis Pedro Almeida<sup>4,5</sup>,  
4 Gerd Masselink<sup>4</sup>, Cai O. Bird<sup>6,2</sup>, Douglas Dodds<sup>7</sup>, Andrew J. Plater<sup>2</sup>

5  
6 1The National Oceanography Centre, Marine Physics and Ocean Climate, Liverpool, UK

7 2University of Liverpool, Department of Geography and Planning, Liverpool, UK

8 3University of Exeter, Medical School, European Centre for Environment and Human Health, Truro  
9 UK

10 4Plymouth University, School of Biological & Marine Sciences Plymouth, UK

11 5Centre National d'Études Spatiales (CNES-LEGOS), Toulouse, France

12 6Marlan Maritime Technologies Ltd, Liverpool, UK

13 7National Grid, Engineering & Asset Management, ETO, Warwick, UK

14 \*Corresponding author's email [jebro@noc.ac.uk](mailto:jebro@noc.ac.uk)

## 15 16 **Highlights**

- 17 • Changing threats to coastal populations and infrastructure are found.
- 18 • Features that enable coastal resilience are identified.
- 19 • An approach to develop a stakeholder-focussed decision-support tool is presented.
- 20 • Physical process understanding and real options analysis are combined.

## 21 22 **Abstract**

23 There is a good understanding of past and present coastal processes as a result of coastal  
24 monitoring programmes within the UK. However, one of the key challenges for coastal managers  
25 in the face of climate change is future coastal change and vulnerability of infrastructure and  
26 communities to flooding. Drawing on a vulnerability-led and decision-centric framework (VL-DC)  
27 a Decision Support Tool (DST) is developed which, combines new observations and modelling to  
28 explore the future vulnerability to sea-level rise and storms for nuclear energy sites in Britain. The  
29 combination of these numerical projections within the DST and a Real Options Analysis (ROA)  
30 delivers essential support for: (i) improved response to extreme events and (ii) a strategy that  
31 builds climate change resilience.

32

33

34 **Key words:** Decision Support Tool (DST); Real Options Analysis (ROA); Flood hazard modelling;  
35 Storm impact monitoring; Human intervention.

36

### 37 1. Introduction

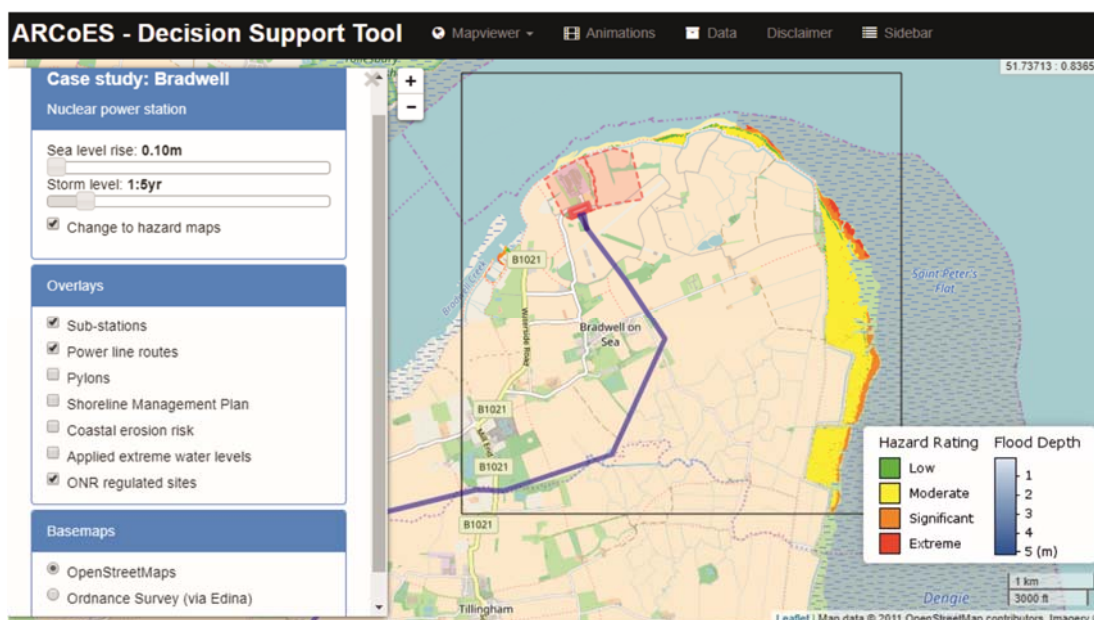
38 Energy security is a fundamental requirement for well-functioning modern societies (Morrissey et  
39 al., 2018). Due to its prevalent location in coastal areas, climate change, sea-level rise and extreme  
40 events represent significant challenges to the global energy infrastructure and supply chain  
41 (Reichl et al., 2013; Morrissey et al., 2018; Prime et al., 2018). The UK Energy Networks  
42 Association (ENA) identifies the biggest pressure to be from coastal flooding - if an electrical  
43 substation is flooded costs in clean up and repair can be high, and on-going costs from disruption  
44 and loss of supply have the potential to add to this significantly (Energy Network Association,  
45 2009). There is already a good understanding of past and present coastal processes, particularly  
46 at locations for present and planned nuclear power stations. However, to ensure that coastal  
47 populations and the necessary infrastructure required to sustain these populations are resilient  
48 in the future, tools that can inform adaptive management are required (Silva et al., 2017; Wadey  
49 et al., 2017; Lam et al., 2017). However, this is a complex problem as shoreline resilience to  
50 changes in the physical environment varies spatially and temporally in response to factors such as  
51 changing beach volume (Castelle et al., 2015), reduction in sediment supply (Guangwei, 2011),  
52 and the degradation of coastal wetlands (Lotzel et al., 2006), as well as to human interventions  
53 that are socio-economically, politically and culturally determined (Ratter et al., 2016). To be  
54 effective, management tools require the capacity to monitor and project a variety of interlinked  
55 physical and societal processes including sea-level rise, storm magnitude/frequency relationships,  
56 changing sediment budget (Brown et al., 2016) and population change and economic activity  
57 (Prime et al., 2018).

58

59 Developed for the UK energy sector as part of the Adaptation and Resilience of Coastal Energy  
60 Supply (ARCoES) project, this paper presents a web-based geospatial Decision-Support Tool (DST),  
61 the ARCoES DST (Fig. 1). Leaflet, an open source Javascript library, is used to construct the DST to  
62 enable the end user to interrogate the matrix of model results using slider bars and tick box  
63 options to toggle between hazard or inundation maps and overlay different infrastructure or map  
64 views (Knight et al., 2015). As described in this paper, the ARCoES DST is used in combination with

65 modelling and monitoring of different coastal environments to better understand future coastal  
66 vulnerability. Drawing on the interdisciplinary skills of the ARCoES researchers, the ARCoES DST is  
67 combined with an economic framework, Real Options Analysis (ROA), to provide an assessment  
68 of when it is most cost-effective to implement a new management approach. From a policy  
69 perspective, the data produced by the DST, when combined with a Real Options Framework can  
70 be used to initiate discussions with coastal practitioners to identify how future vulnerability to  
71 coastal flooding may be mitigated through appropriate and timely intervention and adaptation.  
72 Importantly, although the methodology is designed for the nuclear energy sector, the DST could  
73 also be applied for other coastal management needs.

74



75

76 Fig. 1. The ARCoES DST, available at <http://arcoes-dst.liverpool.ac.uk/>. Flood risk assessments for  
77 ONR regulated sites (shaded) are covered by existing pre-operational and operational safety cases.

78

79 Within this context, the aim of this paper is to demonstrate the usefulness of the ARCoES DST in  
80 understanding the physical and economic impact of sea-level rise and storms across 4 nuclear  
81 energy sites located along the coast of the UK. These sites include Seascale (representing Sellafield  
82 in the northwest), Lilstock (representing Hinkley Point in the southwest), Sizewell (in the east),  
83 and Bradwell (in the southeast). We also focus on Fleetwood (in the northwest) as an example of  
84 its application to a coastal community. The paper continues as follows: the methods used to  
85 deliver this holistic assessment are presented in Section 2. In Section 3 a selection of results to  
86 demonstrate the application and capabilities of the resulting DST at different sites is provided. The

87 way in which this DST can be used to conceptualize shoreline management requirements to pose  
88 questions at a high level for specialized studies to address is discussed in Section 4, before the  
89 conclusions about the future resilience of UK coastal energy are drawn in Section 5.

90

## 91 **2. Site Descriptions**

92 Although applied to a number of locations, here we focus on five study sites with different coastal  
93 geomorphology and hazard exposure. This national application demonstrates the development of  
94 a DST for the management needs of an industry with infrastructure in multiple locations rather  
95 than in response to site-specific coastal conditions. Each site requires a slightly different model  
96 configuration (see Section 3) but uses the same approach.

97

98 The coastline at Seascale/Sellafield faces the Irish Sea, the actual location is quite exposed  
99 (offshore  $H_s, 10\% = 2$  m; max  $H_s = 5.7$  m; data from British Oceanographic Data Centre (BODC) wave  
100 buoy MCMBE-OFF 1974–1976), with a maximum tide range and 1% storm surge height during  
101 winter of 7 m and 1 m, respectively. However, the beach morphology fronting the facility is  
102 characterised by a reflective high tide gravel/cobble beach with an extremely dissipative sandy  
103 intertidal zone. A storm monitored in January 2013 that more or less coincided with spring high  
104 tide had therefore insignificant impact on the beach (Almeida et al., 2014).

105

106 At Lilstock/Hinkley Point, located in the Bristol Channel, the site is not fully exposed to the Atlantic  
107 waves, but wave conditions can be relatively energetic (offshore  $H_s, 10\% = 1.8$  m; max  $H_s = 3.7$  m;  
108 data from BODC wave buoy SEVERNEST A 1979–1981). This is a mega-tidal environment with a  
109 maximum tide range of 10.7 m and a 1% storm surge height during winter of 0.8 m. However, in  
110 common with Sellafield, the wide and low gradient intertidal zone, here a rocky platform instead  
111 of a sandy beach, is extremely dissipative, limiting the wave energy levels impacting the high tide  
112 gravel/cobble beach. A storm monitored in December 2013 had therefore very limited  
113 morphological impact.

114

115 The gravel beach at Sizewell faces the North Sea. Wave conditions are relatively mild (offshore 10%  
116 exceedance  $H_s = 0.6$  m; max  $H_s = 2.2$  m; data from BODC wave buoy ALDEBURG 1975–1977) and  
117 the maximum tide range and 1% storm surge height during winter are 2.4 m and 1 m, respectively.  
118 During the 5-year duration of the ARCoES project, not a single extreme wave event occurred at

119 Sizewell, but some measurements were made during a relatively modest storm event in March  
120 2013. These revealed that the subtidal bar morphology at this site provides significant protection  
121 to the high tide gravel beach from large waves and that the main morphological changes occurred  
122 due to longshore sediment transport processes. The most significant wave events along the North  
123 Sea coast are from the northeast quadrant, but Sizewell is partly sheltered from such storms  
124 because the coastline aligns south-southwest to north-northeast, and potentially the most  
125 damaging waves for Sizewell are extremely rare storm waves from the southeast. Interestingly,  
126 the storm surge event in 2013, and which caused much erosion and flooding along the east coast  
127 of England (Wadey et al., 2015), was not an event of significance at Sizewell where  $H_s$  at the peak  
128 of the storm surge were  $< 1.5$  m.

129

130 The Bradwell site is characterised by a narrow gravel coastal plain fronted by the silty tidal flat and  
131 is located on the southern bank of the Blackwater estuary. The maximum tide range here is 4.8 m  
132 and the 1% winter storm surge is 0.9 m. The site is extremely sheltered and this is demonstrated  
133 by the results of a long-term deployment (Oct 2015 –Mar 2016) of pressure sensors at the base  
134 of the gravel beach and around low tide level. Mean wave conditions were characterised by  $H_s =$   
135 0.1 m and the most energetic event that occurred during this period had a  $H_s$  of 0.45 m.

136

137 Observing the physical processes at the sites above has found that they have a low vulnerability  
138 to storm impact. Seascale/Sellafield and Lilstock/Hinkley Point are relatively exposed sites, the key  
139 aspect limiting their vulnerability to extreme wave events is their highly dissipative intertidal zone  
140 (sand at Sellafield and rock at Hinkley Point). The very wide ( $> 200$  m) and low-gradient ( $< 0.015$ )  
141 surface fronting the high tide gravel/cobble beach and coastal structures at both sites greatly  
142 reduces the wave energy levels and wave runup around high tide, and therefore the risk of  
143 flooding and erosion, even under the largest offshore waves. Sizewell is sited such that it is not  
144 exposed to the most frequent North Sea storm wave conditions from the northeast quadrant. In  
145 addition, the low gradient and barred subtidal zone effectively dissipates storm wave energy, and  
146 the high and wide inter- and supratidal gravel beach also provides a significant buffer to extreme  
147 wave action. The site is perhaps most vulnerable to longer-term coastal dynamics, specifically  
148 alongshore redistribution of sand and gravel due to littoral drift. Bradwell is sited in an extremely  
149 sheltered location with very limited fetch and potential for wave generation. A low gradient  
150 subtidal zone and gravel ridges also fronts the facility, which adds additional protection.

151

152 In addition to sites of nuclear infrastructure the ARCoES DST was also developed to assess  
153 community vulnerability to coastal hazards. Our example site at Fleetwood, northwest England, is  
154 used here to demonstrate how flood hazard management of a community's electricity distribution  
155 has to consider the influence of shoreline management plans on the inland flood hazard to  
156 electricity substations to ensure the supply is resilient. The coastal conditions at this site include  
157 a mega-tidal regime (exceeding 10 m during spring tides), surge events that can reach 2 m and  
158 offshore wave conditions that can exceed 5.5 m (Brown et al., 2010). Our study region has a 'hold  
159 the line' shoreline management policy to protect the community from flood hazards. Within our  
160 study area this policy is implemented by a sea wall, thus understanding when a future 'tipping  
161 point' in wave overtopping hazard may occur for the existing scheme under rising sea levels is  
162 important.

163

### 164 **3. ARCoES DST**

165 There is often a good understanding of past and present coastal processes as a result of coastal  
166 monitoring programmes within the UK. However, one of the key challenges for managers in the  
167 face of climate change, is future coastal change and vulnerability of infrastructure and  
168 communities to flooding. A vulnerability-led and decision-centric framework (VL-DC) (Armstrong  
169 et al., 2015), the ARCoES approach combines new observations and modelling to explore the  
170 future vulnerability to sea-level rise and storms for nuclear energy sites in Britain. As will be  
171 outlined below, the resulting DST provides inundation mapping via LISFLOOD-FP, XBeach, XBeach-  
172 G and SWAB modelling. The data are then combined in a ROA framework to provide an  
173 assessment of when it is most cost-effective to implement a new management approach.

174

#### 175 *3.1 Inundation Mapping*

176 Inundation mapping is a key component of the ARCoES DST. While a general overview of the  
177 model application is provided here, more detailed studies focusing on individual sites (e.g., Prime  
178 et al., 2015a; 2015b; 2016) have considered sensitivity analysis of the model results to ensure the  
179 approach is robust for the purpose of the DST. A "soft" coupling approach is adopted where a  
180 storm impact model provides the input to an inundation model. Here we use models that are  
181 frequently used in flood and erosion risk studies (e.g., Lewis et al., 2013; Phillips et al., 2017; Poate  
182 et al., 2016).

183

184 LISFLOOD-FP (Bates et al., 2005) has been applied as a coastal inundation model to map depth,  
185 extent and velocity of floodwaters for extreme coastal and riverine events under rising sea levels.  
186 The horizontal model resolution varies from 20 m to 50 m depending on the size of the domain  
187 (which range from sites of critical infrastructure to the regional scale for supply network  
188 assessments) to allow efficient computation time and to capture the required level of detail for  
189 the management needs. Data on the time-varying storm tide alone, or combined storm tide and  
190 wave overwashing or overtopping volumes are used to generate the hazard imposed at the coastal  
191 boundary within LISFLOOD-FP, which propagates the floodwater landward across the floodplain.  
192 The positioning of the coastal boundary is domain-dependent as is the boundary input data. At  
193 sites where wave hazard is considered negligible the low water contour is imposed as the coastal  
194 boundary and forced by storm tide water levels at 15 minute time intervals. At sites where wave  
195 hazard is considered important, through overtopping or overwash, the crest of a defence line  
196 (natural or engineered) is set as the coastal boundary and a wave resolving storm impact model  
197 is used to provide the (10 minute average) inflow discharge. In all cases the implemented models  
198 are run for a tidal cycle starting from low water. The inland model boundary is set some distance  
199 from the coast to ensure the flood pathways and area of inundation are generally contained within  
200 the domain. The boundary is set to allow through flow so under very extreme events the water is  
201 not restricted in a way that will cause it to inaccurately build-up. For the Fleetwood case high river  
202 flows have also been imposed as a discharge at the boundary points that cross the river Wyre (see  
203 Prime et al., 2015a). This allows the user to explore a range of flood hazard combinations (sea-  
204 level rise, coastal storms and high river flow).

205

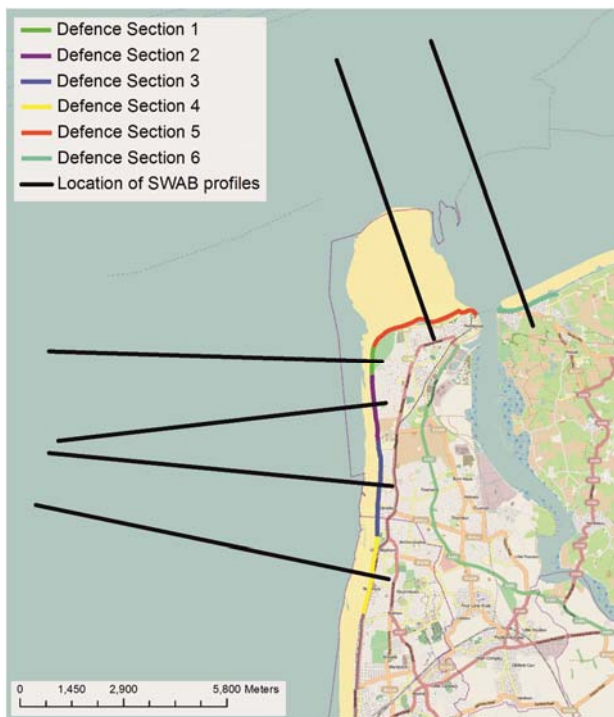
206 At sites with wave hazard, overwashing or overtopping volumes have been calculated for various  
207 defences: hard engineered (SWAB, McCabe et al., 2013), sand dune (XBeach, Roelvink et al., 2010)  
208 or gravel barrier (XBeach-G, McCall et al., 2014, 2015). The use of the XBeach and XBeach-G  
209 models enables the role of storm-driven morphology and features within the cross-shore profile  
210 to be considered within the impact assessment. These models are applied as 1DH (horizontal)  
211 cross-shore profile models for present-day morphologies within the DST, while hypothetical future  
212 morphologies (such as changes in saltmarsh extent, barrier beach morphologies or subtidal bar  
213 geometries) are considered in more focused site-specific applications to determine potential  
214 changes in a system's response to storm impact (e.g., Prime et al., 2015b). The Shallow Water

215 Boussinesq Model (SWAB) has also been used for a site with a sea wall (Prime et al., 2015a).  
216 Although XBeach and XBeach-G can consider a fixed structure within the profile SWAB has been  
217 developed and validated with field observations to account for random wave breaking, impact  
218 and overtopping of sea walls (McCabe et al., 2013).

219

220 The initial profiles in the 1DH simulations are based on a combination of the latest available  
221 bathymetric data and beach profile surveys obtained for the site. The modelled cross-shore  
222 profiles have been selected to capture alongshore variability in the present-day coastal defence.  
223 At sites of energy infrastructure with a natural defence (gravel barrier or dunes) a 1 km spacing  
224 between the profiles with 50 m spacing closer to the nuclear power station is used to capture the  
225 alongshore variability in the beach-barrier system (Prime et al., 2016). For sites with sea walls a  
226 centrally positioned transect perpendicular to each defence section is chosen to simulate the  
227 flood hazard for each of the different defence designs (Prime et al., 2015a). An example set-up is  
228 shown in Fig. 2, where the sea wall provides protection to the local community behind. For sites  
229 where the 1DH models have been used to incorporate wave impact the wave direction is always  
230 assumed to be directly onshore to generate the worst case scenario.

231



232

233 Fig. 2. The LISFLOOD-FP model domain used to simulate flood hazard around the Fylde peninsula,  
234 northwest England. SWAB is applied in this example for each cross-section to simulate the wave-



235 water inflow at the defence crest level (Prime et al., 2015a).

236

237 Within the ARCoES DST the flood maps were developed using data available to coastal managers.  
238 This includes the most recently available airborne laser altimetry (LiDAR) collected by the  
239 Environment Agency (EA) and observational data collected by national monitoring programs  
240 where available. These data include shoreline profile information collected by the EA or local  
241 authorities, the UK tide gauge network record (established in 1953), owned and operated by the  
242 EA, and the WaveNet record, a UK network of wave buoys (established in 2002) operated by the  
243 Centre for Environment Fisheries and Aquaculture Science (CEFAS). These real-time systems  
244 provide a long-term data archive to which a joint probability analysis can be applied to generate  
245 wave-water level combinations representative of a range of storm severities. Where observations  
246 are not available tidal predictions are obtained from the POLTIPS3 software, available from the  
247 national tide sea level facility, and wave data are obtained from long-term (40-year) hindcasts,  
248 such as the UK Climate Predictions 09 (UKCP09, Lowe et al., 2009) and the global wave hindcast  
249 produced in preparation of the European Centre for Medium Range Weather Forecasts (ECMWF,  
250 2016) next reanalysis (ERA5).

251

252 Where observations are limited to within the last decade (e.g., wave monitoring) or where only  
253 waves or water levels are monitored, archived data from climate modelling systems can be utilized  
254 to lengthen the datasets. The longer the data record the greater the confidence in the extreme  
255 value analysis. This research has used the European Centre for Medium-Range Weather Forecasts  
256 (ECMWF) 30-year wave ECWAM cycle 41R1 model data to lengthen the wave records. These  
257 numerical data are validated against existing wave observations prior to use in the analysis.

258

259 For the UK energy sector, events ranging from typical (1:1 year return period) to extreme (1:10,000  
260 year return period) conditions are considered. The joint probability analysis is performed using  
261 JOIN-SEA (Hawkes and Gouldby, 1998). This software uses the generalised Pareto distribution  
262 (GPD) model and simultaneous records of significant wave height ( $H_s$ ) and water level ( $WL$ ) at the  
263 time of the observed high water. In most cases the combined observational record covered a  
264 period of the order of a decade, the limitation often being related to the deployment of the wave  
265 buoy. For each return level a range of wave-water level conditions are generated. These cover  
266 conditions that transition from lower  $WL$  and higher  $H_s$  to higher  $WL$  and lower  $H_s$ . The conditions

267 that pose greatest flood hazard along the probability curves are selected from an ensemble of  
268 1DH storm impact simulations that generate a range of inflow conditions to impose into  
269 LISFLOOD-FP (Prime et al., 2016). This generates the database of flood maps behind the DST. In  
270 this respect, the DST operates as a look-up table.

271

272 Once the required wave-water level combination has been ascertained a storm tide is created to  
273 force the offshore model boundary. The storm tide comprises a spring tide and a surge curve,  
274 available for all UK Class A tide gauge locations from the EA (McMillan et al., 2011). The surge  
275 curve is used to scale the tide such that the total high WL reaches the required extreme value.  
276 The time-varying water levels are combined with the required wave conditions within the 1DH  
277 storm impact model. Although the  $H_s$  is kept constant, a JONSWAP (Joint North Sea Wave  
278 Observation Project) spectrum is applied to create a time-varying wave field. This approach  
279 represents the worst-case scenario as the wave conditions maintain the desired extreme value for  
280 the duration of the simulation, a complete tidal cycle. An appropriate peak wave period ( $T_p$ ) is  
281 selected from the wave data for each  $H_s$ . At many sites around the UK there is a bimodal wave  
282 climate related to the wind sea and swell wave components. For each wave condition the longest  
283  $T_p$  associated with each  $H_s$  is used to simulate the highest wave runup levels.

284

285 Future sea-level projections are incorporated into the still water level of each event to take into  
286 consideration sea-level rise and explore future change in the inundation hazard. The projections  
287 are chosen to represent the high-end emission scenarios up to 2500AD (Jevrejeva et al., 2012).  
288 Incremental increases in mean sea level are considered at 10 cm intervals up to a rise of 2 m and  
289 then at 25 cm intervals to a rise of 5.5 m (Knight et al., 2015). The higher resolution is considered  
290 for levels representing plausible projections that could occur over the next 100 years, consistent  
291 with the long-term shoreline management planning framework. A lower resolution is then applied  
292 for the more bespoke longer term (c. 500 year) projections for the energy industry.

293

294

### 295 *3.2 Monitoring*

296 Alongside the numerical applications, storm surveys were performed at three nuclear sites across  
297 the UK, including Seascale (representing Sellafield in the northwest), Lilstock (representing  
298 Hinkley Point in the southwest) and Sizewell (in the east), as well as a long-term wave gauge

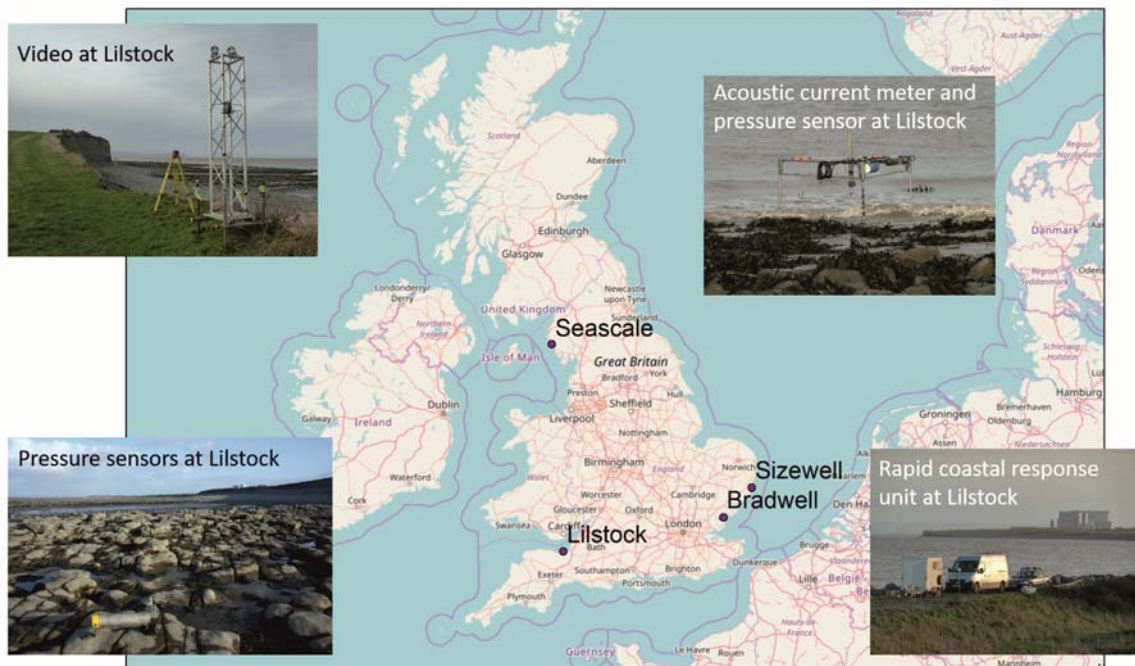
299 deployment at Bradwell (in the southeast). This extreme event monitoring is used to assess the  
300 present-day vulnerability and disturbance-recovery behaviours of the sites. In order to  
301 compliment short-term survey campaigns that aim to characterise coastal response to storms, a  
302 cost-effective method of providing continuous observation of morphological change by  
303 automatically mapping large coastal areas has also been developed using a standard marine  
304 navigational radar (Bell et al., 2016; Bird et al., 2017a).

305

### 306 *3.2.1 Surveys*

307 Storm surveys over a tidal cycle were used to assess the response of different coastal systems and  
308 identify features that make them resilient or resistant to storm impact. During an event pre-,  
309 during and post-storm topographic data were collected (using a dGPS on a staff pole at low tide)  
310 alongside in-situ measurements and remote sensing observations. The in-situ instruments (e.g.,  
311 Fig. 3) were deployed pre-storm and retrieved after the storm. These included two low water  
312 scaffold rigs with pressure transducers and current meters together with five scaffold tubes with  
313 pressure transducers deployed alongshore at equal spacing (< 1 km) on the intertidal terrace.  
314 These instruments recorded the wave and tide elevations and the current velocities during the  
315 storm. Remote sensing techniques included a tower with two video cameras and a second tower  
316 with a laser-scanner. The video cameras were positioned to continuously record alongshore  
317 variability of wave runup during the storm (Poate et al., 2016). The laser-scanner tower was  
318 deployed on the beach face to measure morphological change and swash hydrodynamics along a  
319 cross-shore transect throughout the storm (Almeida et al., 2015; Almeida et al., 2017).

320



321

322 Fig. 3. Location map of the storm survey sites and examples of the instrumented rigs and towers  
 323 deployed.

324

325 *3.2.2 Long-term monitoring*

326 A new monitoring technique has been deployed, which uses a radar-imaged sea surface and an  
 327 accurate record of tidal elevations (such as a nearby tide gauge) as an altimeter to measure tidally-  
 328 driven water level elevations at each pixel in a radar scan. By knowing the position of the waterline  
 329 and the tidal elevation a bathymetric survey of the intertidal area can be produced. This  
 330 methodology was used to observe seasonal changes in morphology over a 3-year period and  
 331 assess storm impacts on beach volume and intertidal bedforms (Bird et al., 2017a). With the  
 332 ambition of applying this radar technique to multiple locations a semi-mobile radar survey system  
 333 has been developed during the ARCoES project by *Marlan Maritime Technologies Ltd*. This system  
 334 is powered by solar panels and a wind turbine and provides a stable radar tower, CCTV camera  
 335 and data recorder, enabling coastlines with limited power infrastructure to be monitored  
 336 effectively. This system continuously monitors beach topography within a few kilometres of the  
 337 radar for the entire duration of the deployment, which can then potentially update intertidal  
 338 bathymetry and waterline levels in near real-time. Study sites are shown in Fig. 4.

339



340

341 Fig. 4. Location map of the radar monitoring sites and the radar systems deployed.

342

343 A previous application to the Dee estuary, northwest England, has demonstrated the capability of  
 344 the radar to monitor complex geomorphological environments (Bird et al., 2017b). The tidal range  
 345 in this estuary is in excess of 10 m on high spring tides. The morphology is very complex and  
 346 includes large areas of intertidal sandflats, subtidal channels, mud banks, saltmarshes and rock  
 347 outcrops. Using a 2.5 m radar antenna intertidal topography was derived with a 3 m spatial  
 348 resolution over a 4 km range from the radar. Comparison with LiDAR showed radar-based system  
 349 was able to derive the major features of the topography including complex channels and bedforms  
 350 with a vertical accuracy of +/- 20 cm (although limitations with the LiDAR data should also be  
 351 acknowledged in any error analysis) (Bell et al., 2016). This surveying system therefore provides  
 352 advanced warning of adverse morphological change, volumetric information on sediment  
 353 movements (especially useful for monitoring beach nourishment schemes or identifying erosion  
 354 hotspots), bedform migration and broad-scale indications of a beach system health. Following the  
 355 development of this rapidly deployable remote-sensing survey platform (Rapidar), planned winter  
 356 deployments at sites of critical energy infrastructure (2017-18 for Minsmere, E coast UK, and  
 357 2018-19 for Dungeness, SE coast UK) will collect data to assess longer-term resilience of these  
 358 sites. These will also be complemented by additional storm surveys to assess the response of

359 these coastal systems to a winter season. This will help to identify and assess the role of shoreline  
360 response and morphological evolution within flood hazard assessments, enabling better  
361 understanding of some of the uncertainty surrounding modelled flood maps.

362

### 363 *3.2.3 Real Options Approach (ROA)*

364 The financial viability of investment projects or the selection of investment alternatives is typically  
365 assessed by cost–benefit analysis. The most widely used method is updating the future cash flows  
366 generated by the coastal scheme. This method is often referred as Discounted Cash Flow (DCF).  
367 However, it is widely acknowledged that the DCF leads to suboptimal decisions when irreversible  
368 investments are subjected to uncertainty (Pringles et al., 2015), such as large-scale infrastructure  
369 investment. Parallel to the modelling and monitoring of the physical processes, a Real Options  
370 Analysis (ROA) was developed to identify which energy infrastructure will benefit from flood  
371 management investment, and the optimal time to invest in this infrastructure (Prime et al., 2018).  
372 ROA is an adaptation of financial options analysis applied to valuing of physical or real assets  
373 (Pringles et al., 2015). ROA assesses the implied value of flexibility that is embedded in many  
374 investment projects. Flexibility acknowledges that investment plans are modified or deferred in  
375 response to the arrival of new (though never complete) information or until the uncertainty is  
376 fully resolved (Pringles et al., 2015). Using Monte Carlo simulation, the ROA values the options to  
377 defer or invest based on a set of pre-defined decision rules and option valuation (see for example  
378 Pringles et al., 2015). The analysis provided by the ROA is used to form a cost-benefit decision-  
379 support tree.

380

381 The next section presents a series of applications of the ARCoES DST to demonstrate the versatility  
382 of information that can be generated for planning coastal adaptation to climate change.

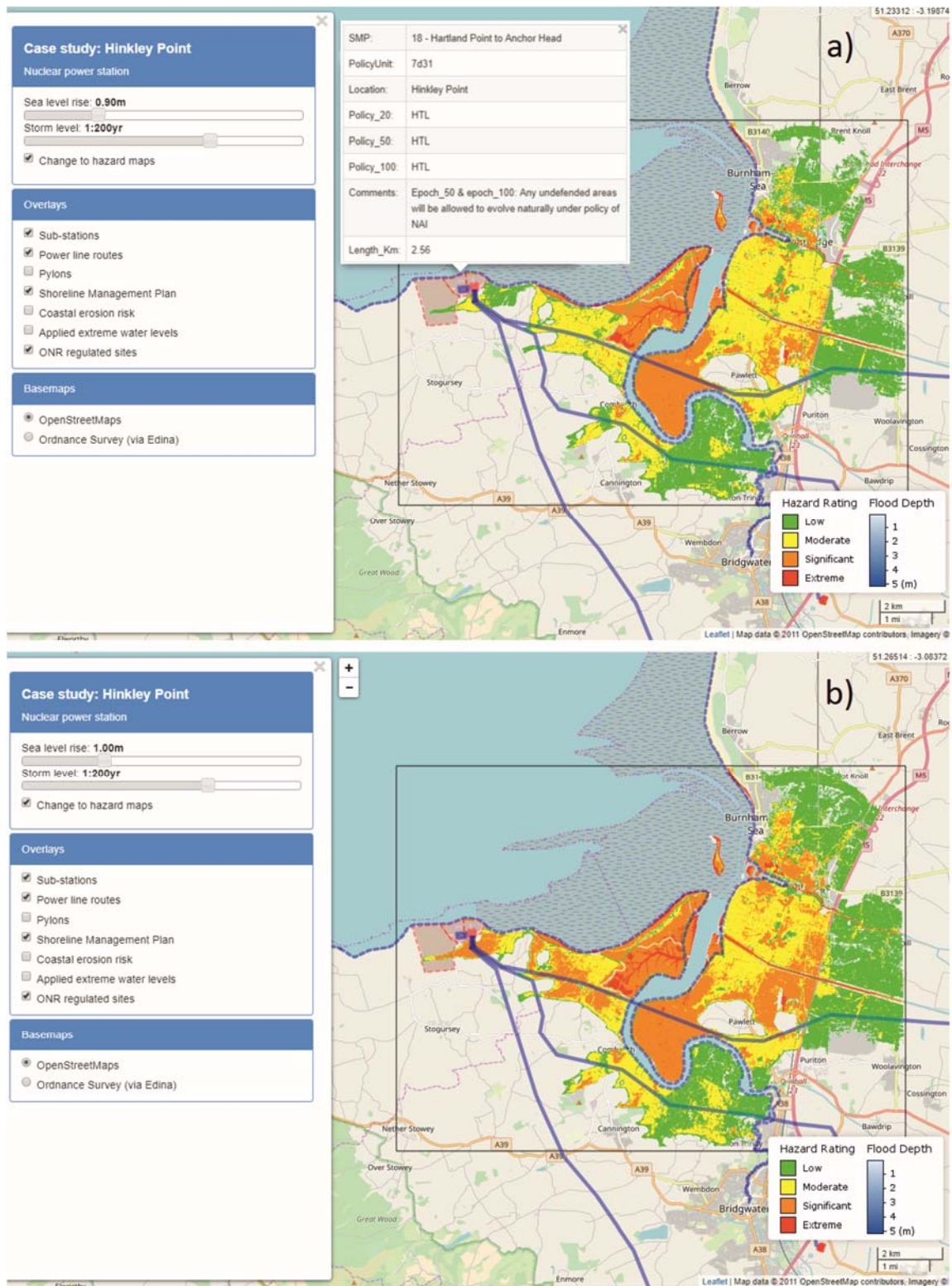
383

## 384 **3. Results**

### 385 *3.1 ARCoES DST*

386 The examples presented use LISFLOOD-FP (alone) in applications within the Bristol Channel and  
387 Severn Estuary, southwest England. At Hinkley Point (Fig. 5) the shoreline management policy is  
388 ‘hold the line’ (HTL Fig. 5a). By selecting a 1:200 year storm condition, typical of UK defence  
389 standards, we identify a tipping point in the storm hazard rating to people (from low/moderate,  
390 Fig. 5a, to significant, Fig. 5b, for road and power line route access) at around 1 m of sea–level

391 rise. At this site the flood hazard occurs due to inundation of lowlands towards the east of the site.  
392 This type of information highlights the need to reassess operational strategies in the future,  
393 particularly for first responders or workers using access routes or working on the electricity  
394 transmission lines.



395

396

397

398

Fig. 5. Hinkley Point, showing a tipping point in the hazard to people from moderate to significant over access and electricity routes for a 1:200 year storm event and a change in mean sea level from a) 0.9 m to b) 1.0 m. Panel a also shows a pop-up window displaying the SMP metadata for



399 a defence section fronting the nuclear power station. Flood risk assessments for ONR regulated  
400 sites (shaded) are covered by existing pre-operational and operational safety cases.

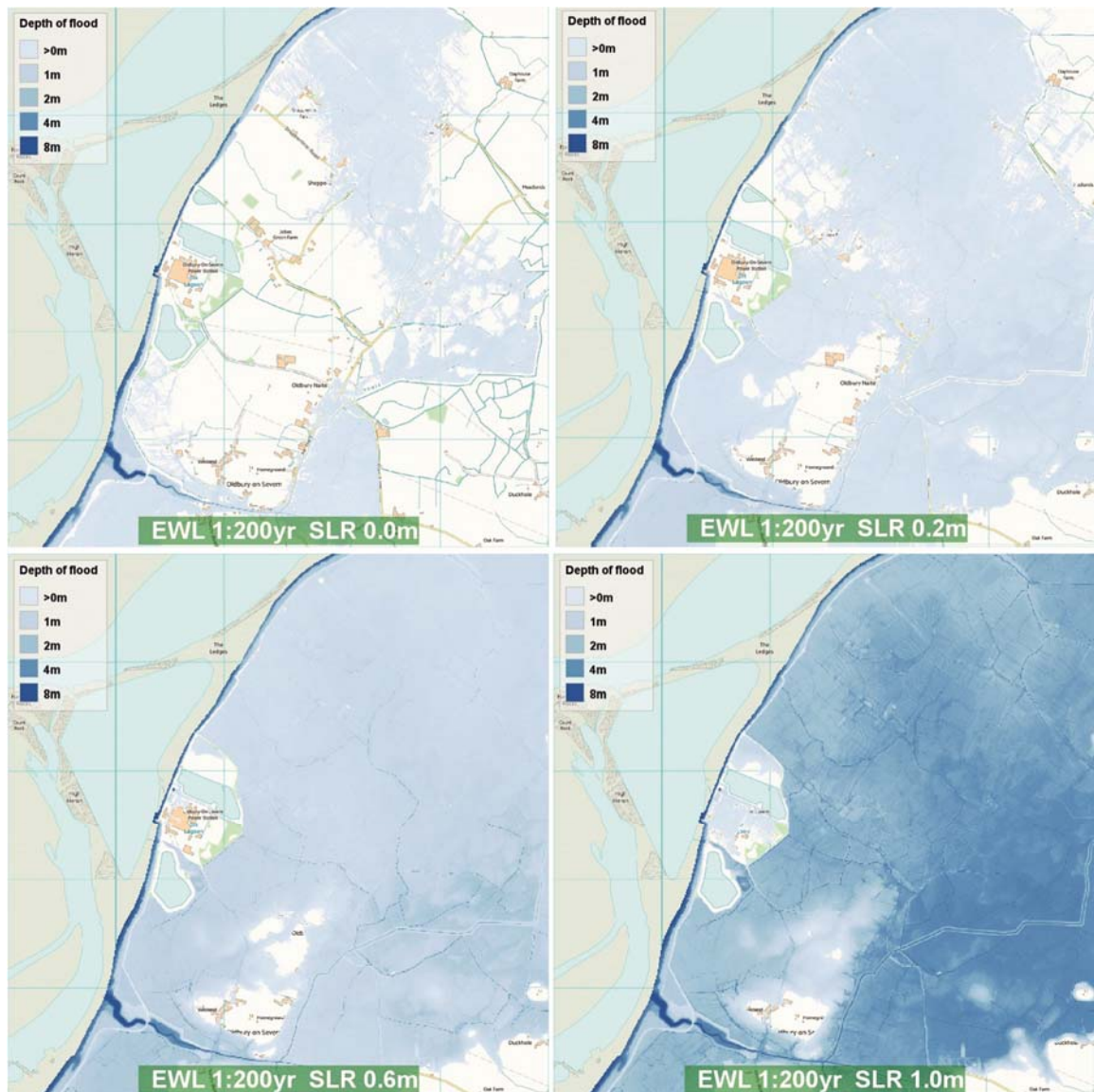
401

402 Animations are also available online for incremental sea-level rise and storm return period for  
403 certain nuclear power station sites. Fig. 6 shows screen shots of the online animations for the  
404 Magnox nuclear power station at Oldbury-on-Severn. The screen shots show increasing sea-level  
405 rise and a constant 1:200 year storm level. The base map used for these images is Ordnance  
406 Survey (OS, 2014). A 1:200 year storm level under present-day sea level (no increase) results in  
407 inundation of agricultural land of less than 1 m. A 1:200 year event, accompanied by 0.2 m sea-  
408 level rise results in more extensive inundation. However, the depth of inundation remains up to 1  
409 m. The Oldbury-on-Severn site remains unaffected, as do some residential properties in the towns  
410 of Oldbury-on-Severn and Oldbury Naite to the south. Around 0.6 m sea-level rise results in a  
411 greater extent of inundation up to 1 m, particularly agricultural land to the southeast of the model  
412 domain. Again, the nuclear site remains unaffected as well as some small areas around Oldbury-  
413 on-Severn. Widespread inundation results from 1.0 m sea-level rise and low lying inland areas  
414 become vulnerable as the flood water propagation is no longer restricted to limited pathways  
415 during tidal high water. All transport and access routes within the area are flooded, as well as local  
416 amenities, agricultural land and residential properties. These images show how the DST can be  
417 used to simulate increasing sea-level rise superimposed on a 1:200 year event and the resulting  
418 depth and extent of inundation, and thus identify where the vulnerability to flooding undergoes  
419 a step change. This information is simulated with no change to present-day flood defence. It can  
420 therefore identify where intervention may be required in the future, showing flood pathways to  
421 help inform the optimal locations to invest in defence infrastructure.

422

423

424



425

426 Fig. 6. Animation screen shot of a scenario with a 1:200 year extreme water level (EWL) and 0.0  
 427 m, 0.2 m, 0.6 m and 1.0 m sea-level rise (SLR) for the Oldbury model domain.

428

429 The DST is currently set-up to provide a simplified estimate of costs calculated from a depth-  
 430 damage curve for different land uses considering inundation by saltwater (Fig. 7a). The DST  
 431 displays the flooded area (km<sup>2</sup>) and cost (£M) for arable land, residential housing, roads, industry  
 432 and the total area of inundation for the selected storm event and sea-level value. Using this  
 433 information appropriate timeframes to implement new management strategies based on the  
 434 relative costs of flooding and the benefits of implementing resilience measures can be planned  
 435 (Prime et al., 2015a).

436

437 *3.2 Real Options Analysis (ROA)*

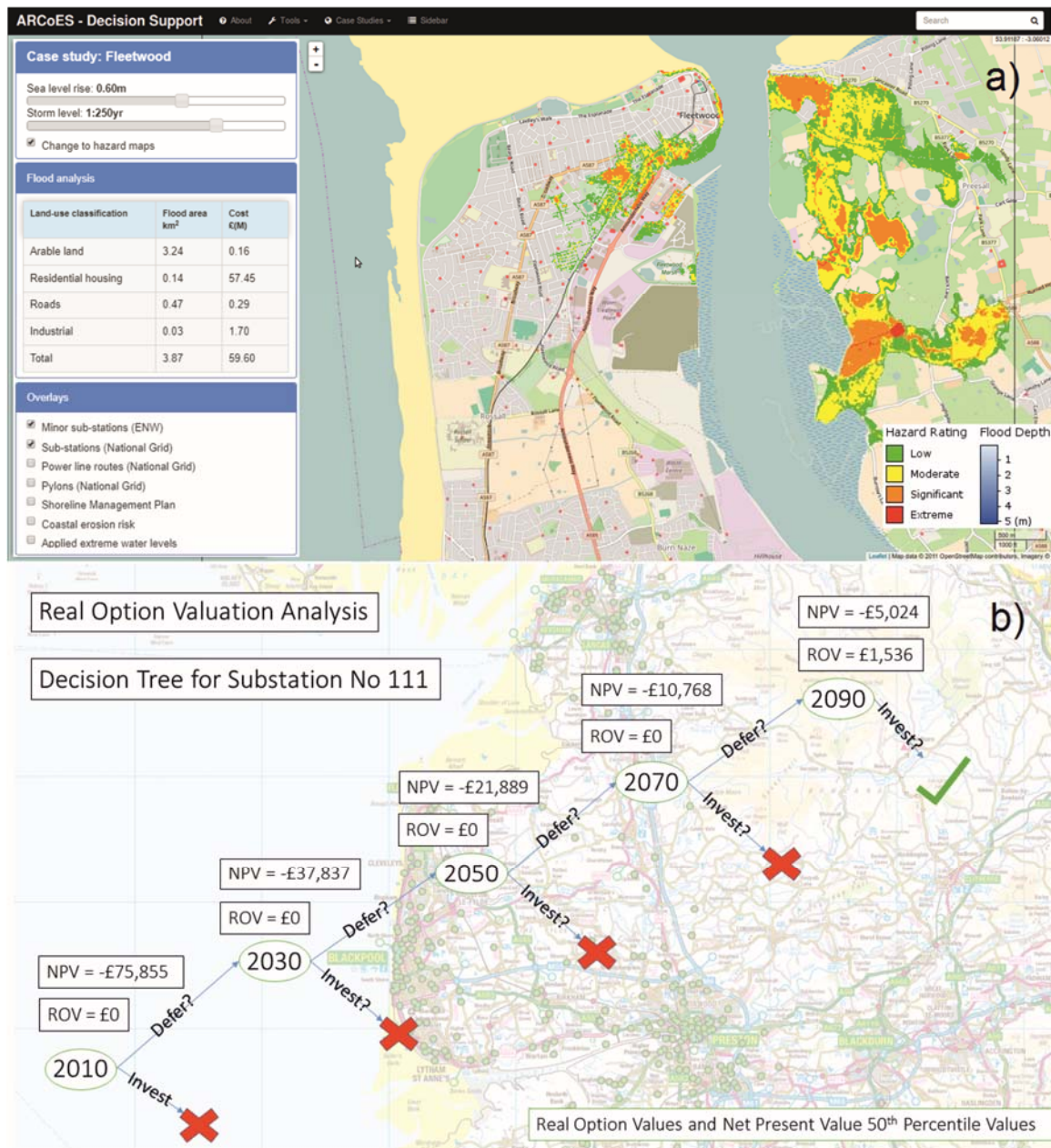
438 By identifying electricity distribution substations that are vulnerable to future flooding using the  
439 DST a ROA can be applied to assess when the implementation of any resilience measures would  
440 be cost-effective. The ROA combines the flood hazard exposure maps simulated for the sea-level  
441 projections with the economic data associated with the investment decision such as inflation,  
442 building costs, maintenance costs, clean-up costs and savings in relation to deferring a project  
443 (Prime et al., 2018). Fig. 7b illustrates a classic Net Present Value (NPV) calculation based on the  
444 most widely used investment decision tool, Discounted Cash Flow (DCF) analysis. According to  
445 DCF-based calculation any substation that has a positive value should go ahead with flood defence  
446 investment. However, NPV calculations based on DCF approaches do not value any flexibility in  
447 the management process. Using ROA a flexible NPV is also calculated. Based on the more flexible  
448 ROA methods, investment in flood defense for substation 111 should only go ahead in 2090.

449

450

451

452



453

454 Fig. 7. Examples of a) the DST cost-benefit information for Fleetwood, northwest England, (the red  
455 symbols indicating where sub-stations are present) and b) the real options analysis decision tree  
456 for a substation in the northwest England.

457

### 458 3.3 Monitoring

459 While the DST explores future scenarios identifying when tipping points in flood hazard for the  
460 current management practice occur and the ROA enables assessment of when it is most cost-  
461 effective to implement a new management approach, observations inform us of the present-day  
462 disturbance-recovery behaviours of coastal environments (cf. Almeida et al., 2015). The ARCoES

463 project found that all four nuclear power station sites that were observed (see Section 2) currently  
464 experience limited vulnerability to extreme storm events due to the combination of their siting  
465 and geomorphology, as well as any site-specific interventions required as part of their pre-  
466 operational and operational safety cases as a requirement of their licencing approval.

467

468 From this understanding we can cast the coastal flooding and erosion risk to nuclear power station  
469 into a Source – Pathway – Receptor framework (Narayan et al., 2012; Sayers et al., 2002) and make  
470 two general statements. Firstly, all nuclear power station locations have limited potential for the  
471 occurrence of extreme wave conditions (i.e., Source) due to their siting. At the same time, the  
472 sites have a common morphology (i.e., Pathway), characterised by a reflective and permeable  
473 gravel/cobble high tide beach fronted by a wide and low gradient dissipative feature. This ensures  
474 that even if the site experiences extreme wave energy levels, potential damage to the nuclear  
475 power station site (i.e., Receptor) due to flooding and erosion would be limited. With uncertainty  
476 surrounding the consequence of climate change and sea-level rise (the Source) at the coast,  
477 monitoring of the morphology (Pathway) is recommended, using techniques such as Rapidar, to  
478 provide early warning to trigger a review of the current management strategy to maintain the  
479 required standard of protection (to the Receptor). Through understanding of the present-day  
480 processes, critical evolution within the system can be identified for consideration in sensitivity  
481 modelling using the models that make up the DST. One example would be the update and  
482 exploration of time-evolving beach profiles within the numerical approach that generates the  
483 hazard maps. Such studies continued study will highlight areas for continued development within  
484 the DST.

485

#### 486 **4. Conclusions**

487 The ARCoES DST and parallel ROA presented in this paper provide a resource that can be used to  
488 initiate discussions with coastal practitioners to identify how future vulnerability to coastal  
489 flooding may be mitigated through appropriate and timely intervention and adaptation. Such a  
490 forum for dialogue is required to improve the transfer of knowledge between coastal researchers  
491 and decision-makers, to enable science based evidence to underpin choices made when setting  
492 new coastal management strategies. The DST enables maps of potential flooding, and associated  
493 costs, from increments of sea-level rise and storm magnitude to be explored by a wide range of  
494 users to identify key locations and ‘tipping points’ where and when the increased vulnerability to

495 flooding challenges current operations, emergency plans and long-term management strategy.  
496 When combined with understanding gained from present day observations informed monitoring  
497 programmes to support management decisions can be put in place and site inspections can be  
498 focused on assessing geomorphic change that has the potential to change a sites vulnerability to  
499 storm impact. The detailed understanding of the local processes also allows the limitations of the  
500 'static' morphology within the DST to be put in context though the identification of how  
501 uncertainty within the mapped results could occur. A key area for expansion of the ARCoES  
502 framework would be to incorporate shoreline evolution within the projections of future coastal  
503 flood hazard. By using freely accessible models and mapping systems within the DST continued  
504 development can be facilitated, enabling incorporation of such information in the future.

505

506 Within a policy context, project outputs have already provided practice and policy  
507 recommendations for national and regional decision-makers on building coastal resilience to sea-  
508 level rise and storms (please see the Living With Environmental Change (LWEC) partnership policy  
509 and practice notes, Plater and Brown, 2016). In this respect, the DST and associated resources  
510 provide a framework for engagement and dialogue across research and stakeholder communities  
511 for the co-production of future plans (e.g., Armstrong et al., 2015). Over the longer term, the DST  
512 provides energy infrastructure stakeholders with a roadmap for planned investments that address  
513 resilience to future change in sea level and extreme events. This would include measures such as  
514 the relocation of substations, raising transformers and other hardware above ground, and  
515 replacing ageing assets (e.g. circuit breakers) that may be more sensitive to water. The DST  
516 therefore delivers essential support for: (i) improved response to extreme events and (ii) a strategy  
517 that builds climate change resilience. Both offer the consumer greater confidence in the constancy  
518 of energy supply and an awareness that their money is being spent effectively in combating  
519 present and future risks from flooding.

520

521 Finally, the ARCoES DST platform is an effective example of inter-disciplinary collaboration across  
522 physical, natural, and social sciences on one axis, and across research, energy and infrastructure  
523 sectors, coastal management authorities, environmental regulators, and coastal communities on  
524 another. Interactive dissemination of the DST has revealed its value in discussions that centre on:  
525 (i) future changes in coastal geomorphology and how this may be managed to promote 'natural'  
526 coastal resilience, (ii) engagement of stakeholders with projections of flooding due to sea-level

527 rise and other forcing factors, and uncertainties therein; and (iii) interventions that mitigate  
528 impacts in an appropriate (according to location and scale of challenge), timely and cost-effective  
529 way. The DST is therefore presented as a resource for framing dialogue and exploring solutions,  
530 rather than providing simplistic answers out of context. Rather than this being viewed in negative  
531 terms by decision makers, the DST has been received positively as providing a focus for the sharing  
532 of knowledge, perspectives and priorities.

533

### 534 **Acknowledgements**

535 This research was funded through the ESRC-funded ARCC ARCoES project (EPSRC EP/I035390/1),  
536 NERC-funded project “Sandscaping for Mitigating Coastal Flood and Erosion Risk to Energy  
537 Infrastructure on Gravel Shorelines: a case study approach” (NE/M008061/1), and the EPSRC IAA  
538 (Impact Acceleration Account) scheme, which funded the project ‘Use of Sandscaping  
539 Interventions for Coastal Protection’. It builds on conference presentations given at Coastal  
540 Dynamics 2017 in Denmark by Brown et al. (2017) and Lyddon et al. (2017). National Grid are also  
541 thanked for their support and input to the development of the DST and for sharing knowledge in  
542 relation to climate change and adaptation. Multiple projects associated to ARCoES have also  
543 contributed to the new understanding and information behind the DST. The key PhD studentships  
544 include: “The feasibility of mega-recharge projects for coastal resilience: physical, economic and  
545 societal considerations” and “Physical, operational and economic resilience of coastal energy  
546 networks.” We would like to thank Jean-Raymond Bidlot from the ECMWF for the provision of the  
547 30-year wave ECWAM cycle 41R1 model hindcast dataset. In addition, we thank CEFAS for  
548 providing the full datasets from WaveNet, and the National Tidal and Sea Level Facility for  
549 providing the tide gauge data archived with the BODC.

550

### 551 **References**

- 552 Almeida, L.P., Masselink, G., McCall, R., Russell, P., 2017. Storm overwash of a gravel barrier: field  
553 measurements and XBeach-G modelling. *Coastal Engineering*, 120, 22–35.
- 554 Almeida, L.P., Masselink, G., Russell, P., Davidson, M., McCall, R., Poate, T., 2014. Swash zone  
555 morphodynamics of coarse-grained beaches during energetic wave conditions. In:  
556 Proceedings of the International Conference on Coastal Engineering, Seoul, South Korea,  
557 2014.
- 558 Almeida, L.P., Masselink, G., Russell, P., Davidson, M., 2015. Observations of gravel beach

559 dynamics during high energy wave conditions using a laser scanner. *Geomorphology*, 228,  
560 15–27.

561 Armstrong, J., Wilby, R., Nicholls, R.J., 2015. Climate change adaptation frameworks: an evaluation  
562 of plans for coastal Suffolk, UK. *Natural Hazards Earth System Science*, 15, 2511–2524.

563 Bates, P.D., Dawson, R.J., Hall, J.W., Horritt, M.S., Nicholls, R.J., Wicks, J., 2005. Simplified two-  
564 dimensional numerical modelling of coastal flooding and example applications. *Coastal*  
565 *Engineering*, 52 (9), 793–810.

566 Bell, P.S., Bird, C.O., Plater, A.J., 2016. A temporal waterline approach to mapping intertidal areas  
567 using X-band marine radar. *Coastal Engineering*, 107, 84–101.

568 Bird, C.O. Bell, P.S. Plater, A.J., 2017a. Application of marine radar to monitoring seasonal and  
569 event-based changes in intertidal morphology. *Geomorphology*, 285, 1–15.

570 Bird, C., Sinclair, A., Bell, P., 2017b. Radar-based nearshore hydrographic monitoring. *Hydro*  
571 *International*, 21(2), 19–21, available online at [https://www.hydro-](https://www.hydro-international.com/content/article/radar-based-nearshore-hydrographic-monitoring)  
572 [international.com/content/article/radar-based-nearshore-hydrographic-monitoring](https://www.hydro-international.com/content/article/radar-based-nearshore-hydrographic-monitoring)  
573 [assessed 27<sup>th</sup> October 2017].

574 Brown, J.M., Knight, P., Prime, T., Phillips, B., Lyddon, C., Leonardi, N., Morrissey, K., Plater, A.J.,  
575 2017. Science based tools informing coastal management in a changing climate.  
576 *Proceedings Coastal Dynamics*, ASCE, Helsingør, Denmark, 12-16 June 2017, 12pp.

577 Brown, J.M., Phelps, J.J.C, Barkwith, A., Hurst, M.D., Ellis, M.A., Plater, A.J., 2016. The effectiveness  
578 of beach mega-nourishment, assessed over three management epochs. *Journal of*  
579 *Environmental Management*, 184 (2), 400–408.

580 Brown, J.M., Souza, A.J., Wolf, J., 2010. An 11-year validation of wave-surge modelling in the Irish  
581 Sea, using a nested POLCOMS-WAM modelling system. *Ocean Modelling*, 33, 118–128.

582 Castelle, B., Marieu, V., Bujan, S., Splinter, K.D., Robinet, A., Sénéchal, N., Ferreira, S., 2015. Impact  
583 of the winter 2013–2014 series of severe Western Europe storms on a double-barred sandy  
584 coast: beach and dune erosion and megacusp embayments. *Geomorphology*, 238, 135–148.

585 ECMWF. 2016. European Centre for Medium Range Weather Forecasts. IFS Documentation,  
586 European Centre for Medium Range Weather Forecasts: Reading, UK.

587 Energy Networks Association, 2009. ENA Annual Review. 26pp, available online at  
588 <http://www.energynetworks.org/assets/files/news/publications/ENARReview2009.pdf>  
589 [Accessed 24 January 2018].

590 Guangwei, H., 2011. Time lag between reduction of sediment supply and coastal erosion.



591 International Journal of Sediment Research, 26 (1), 27–35

592 Hawkes, P.J., Gouldby, B.P., 1998. The joint probability of waves and water levels: JOIN-SEA User  
593 manual V1.0.

594 Jevrejeva, S., Moore, J.C., Grinsted, A., 2012. Sea level projections to AD2500 with a new  
595 generation of climate change scenarios. *Glob. Planet. Change*, 80: 14–20.

596 Knight, P.J., Prime, T., Brown, J.M., Morrissey, K., Plater, A.J., 2015. Application of flood risk  
597 modelling in a web-based geospatial decision support tool for coastal adaptation to climate  
598 change. *Nat. Hazards Earth Syst. Sci.*, 15: 1457-1471.

599 Lam, J.S., Liu, C., Gou, X. 2017. Cyclone risk mapping for critical coastal infrastructure: Cases of  
600 East Asian seaports. *Ocean & Coastal Management*, 141, 43–54.

601 Lewis, M., Bates, P., Horsburgh, K., Neal, J., Schumann, G., 2013. A storm surge inundation model  
602 of the northern Bay of Bengal using publicly available data. *Quarterly Journal of the Royal  
603 Meteorological Society*, 139 (671), 358–369.

604 Lotzel, H.K., Lenihan, H.S., Bourque, B.J., Bradbury, R.H., Cooke, R.G., Kay, M.C., Kidwell, S.M., Kirby,  
605 M.X., Peterson, C.H., Jackson, J.B.C., 2006. Depletion, Degradation, and Recovery Potential  
606 of Estuaries and Coastal Seas. *Science*, 312 (5781), 1806 –1809.

607 Lowe J, Howard T, Pardaens A, Tinker J, Holt J, et al. (2009) UK Climate Projections science report:  
608 Marine and coastal projections, available online at <http://nora.nerc.ac.uk/9734/> [Accessed  
609 20 June 2014].

610 Lyddon, C., Knight, P., Leonardi, N., Brown, J.M., Plater, A.J., 2017. Flood Hazard Sensitivity to  
611 Storm Surge-High Water Concurrence in a Hyper-Tidal Estuary. *Proceedings of Coastal  
612 Dynamics*, ASCE, Helsingør, Denmark, 12pp.

613 McCabe, M.V., Stansby, P.K., Apsley, D.D., 2013. Random wave runup and overtopping a steep sea  
614 wall: Shallow-water and Boussinesq modelling with generalised breaking and wall impact  
615 algorithms validated against laboratory and field measurements. *Coastal Engineering*, 74:  
616 33–49.

617 McCall, R.T., Masselink, G., Poate, T.G., Roelvink, J.A., Almeida, L.P., 2015. Modelling the  
618 morphodynamics of gravel beaches during storms with XBeach-G. *Coastal Engineering*, 103:  
619 52–66.

620 McCall, R.T., Masselink, G., Poate, T.G., Roelvink, J.A., Almeida, L.P., Davidson, M., Russell, P.E.,  
621 2014. Modelling storm hydrodynamics on gravel beaches with XBeach-G, *Coastal  
622 Engineering*, 91: 231–250.

623 McMillan, A., Batstone, C., Worth, D., Tawn, J., 2011. Coastal flood boundary conditions for UK  
624 mainland and islands. Project SC060064/TR2: Design sea levels.

625 Morrissey, K., Plater, A., Dean, M., 2018. The cost of electric power outages in the residential  
626 sector: A willingness to pay approach. *Applied Energy*, 212, 141–50.

627 Narayan, S., Hanson, S., Nicholls, R. J., Clarke, D., Willems, P., Ntegeka, V., Monbaliu, J., 2012. A  
628 holistic model for coastal flooding using system diagrams and the Source-Pathway-Receptor  
629 (SPR) concept. *Natural Hazards and Earth System Science*, 12, 1431–1439.

630 Phillips, B., Brown, J., Bidlot, J.-R., Plater, A., 2017. Role of beach morphology in wave overtopping  
631 hazard assessment. *Journal of Marine Science and Engineering*, 5 (1), 18 pp.

632 Plater, A.J., Brown, J.M., 2016. Building coastal resilience to sea-level rise and storms in the UK.  
633 *Living With Environmental Change, Policy and Practice Note 30*, May 2016, 4pp,  
634 [www.nerc.ac.uk/research/partnerships/lwec/products/ppn/ppn30/](http://www.nerc.ac.uk/research/partnerships/lwec/products/ppn/ppn30/) [assessed 20<sup>th</sup> Feb  
635 2017].

636 Poate, T.G., McCall, R.T., Masselink, G. 2016. A new parameterisation for runup on gravel beaches.  
637 *Coastal Engineering*, 117, 176–190.

638 Prime, T., Brown, J.M., Plater, A.J., 2015a. Physical and economic impacts of sea-level rise and low  
639 probability flooding events on coastal communities. *PLOS ONE*, 10 (2),  
640 e0117030.10.1371/journal.pone.0117030.

641 Prime, T., Brown, J.M., Plater, A.J., Dolphin, T., Fernand, L., 2015b. Morphological Control on  
642 Overwashing Hazard at Multiple Energy Generation Installations. 14th International  
643 workshop on wave hindcasting and forecasting and 5<sup>th</sup> Coastal hazards symposium, 8 - 13  
644 November 2015, Key West, United States, 9pp, available online at  
645 <http://www.waveworkshop.org/14thWaves/index.htm> [Accessed 24 January 2018].

646 Prime, T., Brown, J.M., Plater, A.J., 2016. Flood inundation uncertainty: The case of a 0.5% annual  
647 probability flood event. *Environmental Science and Policy*, 59, 1–9.

648 Pringles, R., Olsina, F., Garcés, F., 2015. Real option valuation of power transmission investments  
649 by stochastic simulation. *Energy Economics*, 47, 215–26.

650 Prime, T., Morrissey, K., Brown, J., Plater, A., 2018. Protecting Energy Infrastructure against the  
651 Uncertainty of Future Climate Change: A Real Options Approach, *Journal of Ocean and  
652 Coastal Economics*, 5 (1), Article 3, 36pp.

653 Ratter, B.M.W., Petzold, J., Sinane, K., 2016. Considering the locals: coastal construction and  
654 destruction in times of climate change on Anjouan, Comoros. *Natural Recourses Forum*, 40,

655 112–126.

656 Reichl, J., Schmidthaler, M., Schneider, F., 2013. The value of supply security: the costs of power  
657 outages to Austrian households, firms and the public sector. *Energy Economics*, 36, 256–61.

658 Roelvink, D., Reniers, A., Van Dongeren, A., Van Thiel de Vries, J., Lescinski, J., McCall, R., 2010.  
659 XBeach model description and manual. Unesco-IHE Inst. Water Educ. Deltares Delft Univ.  
660 Technology.

661 Sayers, P.B., Hall, J.W., Meadowcroft, I.C., 2002. Towards risk-based flood hazard management in  
662 the UK. *Proceedings of the Institution of Civil Engineers*, 150, 36–42.

663 Silva, S.F., Martinho, M., Capitão, R., Reis, T., Fortes, C.J., Ferreira, J.C., 2017. An index-based  
664 method for coastal-flood risk assessment in low-lying areas (Costa de Caparica, Portugal).  
665 *Ocean & Coastal Management*, 144, 90–104.

666 Wadey, M.P., Cope, S.N., Nicholls, R.J., McHugh, K., Grewcock, G., Mason, T., 2017. Coastal flood  
667 analysis and visualisation for a small town. *Ocean & Coastal Management*, 116, 237–247.

668 Wadey, M., Haigh, I.D., Nicholls, R.J.; Brown, J.M., Horsburgh, K., Carroll, B., Gallop, S., Mason, T.,  
669 Bradshaw, E., 2015. A comparison of the 31 January–1 February 1953 and 5–6 December  
670 2013 coastal flood events around the UK. *Frontiers in Marine Science*, 2.  
671 84.10.3389/fmars.2015.00084.